

Polymer Chemistry

Accepted Manuscript



This is an *Accepted Manuscript*, which has been through the Royal Society of Chemistry peer review process and has been accepted for publication.

Accepted Manuscripts are published online shortly after acceptance, before technical editing, formatting and proof reading. Using this free service, authors can make their results available to the community, in citable form, before we publish the edited article. We will replace this *Accepted Manuscript* with the edited and formatted *Advance Article* as soon as it is available.

You can find more information about *Accepted Manuscripts* in the [Information for Authors](#).

Please note that technical editing may introduce minor changes to the text and/or graphics, which may alter content. The journal's standard [Terms & Conditions](#) and the [Ethical guidelines](#) still apply. In no event shall the Royal Society of Chemistry be held responsible for any errors or omissions in this *Accepted Manuscript* or any consequences arising from the use of any information it contains.

Cite this: DOI: 10.1039/c0xx00000x

www.rsc.org/xxxxxx

ARTICLE TYPE

Mesogen-Jacketed Liquid Crystalline Polymers with Peripheral Oligo (ethylene oxide) Chains: Phase Structure and Thermo-responsive Behavior

Qian Tan, Junqiu Liao, Sheng Chen*, Ya Zhu, Hailiang Zhang*

Received (in XXX, XXX) Xth XXXXXXXXX 20XX, Accepted Xth XXXXXXXXX 20XX
DOI: 10.1039/b000000x

A series of mesogen-jacket liquid crystalline polymers carrying the different repeating unit number of oligo(ethylene oxide) (EO) group ($m=1, 2, 3$) and numbers of EO terminal chain (mono, di and tri) have been prepared via free radical polymerization, namely poly{2, 5-bis[(4-methoxyoligo(oxyethylene)benzyl)oxycarbonyl]styrene} (P-mono-mEOBCS), poly{2, 5-bis[(3, 5-dimethoxyoligo(oxyethylene)benzyl)oxycarbonyl]styrene} (P-di-mEOBCS), and poly{2, 5-bis[(3, 4, 5-trimethoxyoligo(oxyethylene)benzyl)oxycarbonyl]styrene} (P-tri-mEOBCS). The chemical structures of monomers were confirmed by ^1H NMR, ^{13}C NMR and Mass Spectrometry. The characterization of the polymers was performed with ^1H NMR, GPC and TGA. The phase structures and transition behaviors were studied using DSC, POM and 1D/2D WAXD. The thermo-responsive behavior was investigated with turbidity measurements using UV-vis spectroscopy. The results showed that P-mono-mEOBCS formed the isotropic phase and were not water soluble. For P-di-mEOBCS, when $m=1$, the polymer exhibited the hexagonal columnar (Φ_{H}) phase and was insoluble. When $m=2$, it presented Φ_{H} phases and the lower critical solution temperature (LCST) of polymer was $23\text{ }^\circ\text{C}$ (10 mg mL^{-1}). When $m=3$, it showed columnar nematic (Φ_{N}) phase and the LCST was $40\text{ }^\circ\text{C}$. For P-tri-mEOBCS, all polymers exhibited the Φ_{H} phase and the LCST increased from 22 to $60\text{ }^\circ\text{C}$ with increasing m . All of those indicated that the jacking effect and hydrophilicity of polymers increased with increasing the numbers of EO peripheral chain. Meantime, the jacking effect decreased and hydrophilicity increased with the increasing of the EO chain length.

Introduction

In the recent years, stimuli-responsive polymers have attracted much interest because of their potential applications in areas such as drug delivery system, biosensors, rheological control additives and separations processes.¹⁻⁶ These stimuli-responsive polymers can change their physical properties (from a hydrophobic to a hydrophilic state) in response to external stimuli such as temperature, pH, electric field, light.⁷⁻¹⁴ Among various external stimuli, temperature is one of the most widely used in

environmentally responsive polymer systems. In aqueous solution, thermo-responsive polymers collapse above their lower critical solution temperature (LCST) because of dehydration of the polymer chains, and subsequently form aggregates. In general, thermo-responsive homopolymers have a repeat unit that contains hydrophilic and hydrophobic moieties. The best known examples of synthetic thermo-responsive polymers are poly(*N*-isopropylacrylamide) (PNIPAm)¹⁵⁻¹⁹ and polyethylene glycol (PEG)²⁰ because of their biocompatibility. Moreover, oligo(ethylene oxide) (EO) is widely used as a common side-chain unit in various polymers, such as polylactides,²¹ polymetacrylates,²² polyacrylates,²³ polypeptide,²⁴ poly(vinylether),²⁵ polystyrenes,²⁶ polyisocyanide²⁷ and polyisocyanate²⁸ because the thermo-responsive property can be controlled by tuning the repeating unit number of EO group. Thus, there are many efforts in the design, synthesis, and application of thermo-responsive polymers based on EO group.

Dendronized polymers have attracted much attention not only in the bulk system but also in the solution.²⁹⁻³² Dendronized polymers are worm-like macromolecules constructed by a linear polymer backbone surrounded with certain structural dendrons at each repeating unit.³²⁻³⁴ The molecular architecture of these

Key Laboratory of Polymeric Materials and Application Technology of Hunan Province, Key Laboratory of Advanced Functional Polymer Materials of Colleges, Universities of Hunan Province, College of Chemistry, Xiangtan University, Xiangtan 411105, Hunan Province, China. Email: huaxuechensheng@163.com, zh11965@xtu.edu.cn

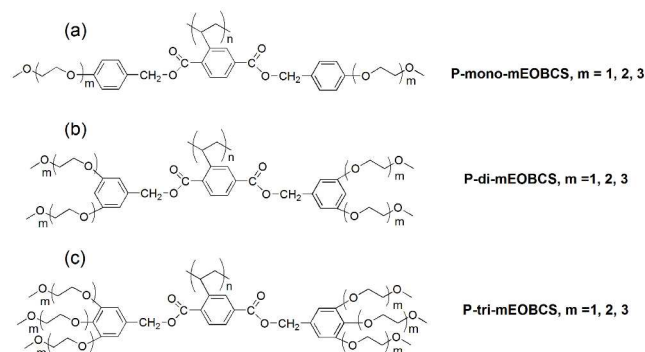
† Electronic Supplementary Information (ESI) available: The characterization data of monomers; ^1H NMR spectra of intermediate products of monomer (mono-1EOBCS); 1D WAXD patterns of the polymer during the second heating process and the second cooling process; 2D WAXD patterns of a sheared P-di-2EOBCS sample. See DOI: 10.1039/b000000x/

macromolecules can be tailored with respect to dendron kinds, size and generation, providing a high level of control over rigidity and functionality. For example, Percec have studied detailedly the self-assembly of dendronized polymers through changing the degree of polymerization of the backbone, the composition of the self-assembling dendron, and the connection between the dendron and the backbone.^{35, 36} In the solution system, much attention has been paid to developing novel thermoresponsive polymers on the basis of dendronized polymers. Most of them were constructed by attaching thermoresponsive units to the “surface” of these dendritic macromolecules. For example, Zhang and Schlüter have researched the thermoresponsive behavior and aggregation of dendronized polymers with oligo(ethylene oxide) (EO) dendrons.³⁷⁻³⁹ The results showed that the thermoresponsive dendronized polymer undergoes a sharp, fast and fully reversible phase transition in aqueous solution.

In late 1980s, Zhou proposed a kind of liquid crystalline polymers, distinguishing themselves from traditional side-chain liquid crystalline polymers and main-chain liquid crystalline polymers, namely the mesogen-jacketed liquid crystalline polymers (MJLCPs) with a short spacer or a single covalent bond connecting the bulky side group to the polymer backbone.^{40, 41} Due to the strong coupling between the polymer main chain and the highly crowded, rigid, and bulky side groups, the macromolecules have to take an extended and stiffened conformation and order into mesophases as a whole as in main-chain liquid crystalline polymers.⁴²⁻⁴⁷ Due to those properties, it is easy to control the rod length by the molecular weights of the MJLCPs. Moreover, the diameter and surface chemistry of the rod can be tuned by altering the structure of laterally attached mesogens, which are very useful in soft matter self-assembly.^{47, 48} In MJLCPs systems, at present, the surface of the rod are basically the nonpolar alkyl chains which are connecting to the mesogens as the flexible terminal groups.^{49, 50} There are only few other kinds of terminal groups to be reported. Such as, Ober *C. et al.* have researched the synthesis and characterization of fluorinated MJLCPs as surface-modifying agents.⁵¹ Fan *et al.* also have studied the influence of fluorinated substituent on the phase behavior of MJLCPs with a biphenyl mesogen.⁵² Chen *et al.* have reported the synthesis and phase structures of MJLCPs substituted with oligo(oxyethylene) as peripheral chain.⁵³ The results showed that all the polymers were chemically and mesomorphically thermally stable.

The MJLCPs and dendronized polymers are both rigid polymers, however, there are no reports on the synthesis of a water-soluble MJLCPs as a novel stimuli-responsive material based on EO-covered pendant dendrons. In this paper, we report on the synthesis of a series of MJLCPs carrying the different repeating unit number of OE group and the structures of polymers are shown in Scheme 1. They are referred as P-mono-mEOBCS, P-di-mEOBCS and P-tri-mEOBCS (*m* is the repeating unit number of EO group, *m*=1, 2, 3). Contrast to the molecular structure of previous MJLCPs,⁵⁴ our design polymers' molecular structure has two distinctive features. One is that side chain is semirigid side chain because of one methylene unit between the alkoxybenzene unit and the oxycarbonyl styrene unit of poly {2, 5-bis [(4-methoxyphenyl)oxycarbonyl] styrenes} (PMPCS) to break the rigidity of side-chain mesogen. Two is that surface

groups are EO terminal groups. We choose EO as the polymers' surface because EO groups exhibit polarity, flexibility and hydrophilicity, moreover, the hydrophilicity can be controlled by tuning the repeating unit number of EO group and the numbers of EO terminal groups (mono, di and tri). Therefore, the aim of the paper is to report results on the investigations of (i) the effects of the semirigid side chain with different the repeating unit number of EO group (*m*=1, 2, 3) and numbers of EO terminal groups (mono, di and tri) on the phase structure and the ability of mesophase formation, (ii) the influence of the number and length of terminal EO chain for the monomers and polymers on the thermoresponsive behaviour and the solubility in water.



Scheme 1 Molecular structure of the mesogen-jacket liquid crystalline polymer.

Results and discussion

Synthesis and characterization of monomers

Monomers were synthesized by the reaction of 2-vinylterephthaleic acid and corresponding Methoxyoligo(ethylene oxide) phenyl methanol in the presence of DCC and DMAP in CH_2Cl_2 . All monomers were thoroughly purified by silica gel column chromatography. The resulting monomer molecular structures were confirmed by ^1H NMR, ^{13}C NMR, and mass spectroscopy. The monomers mono-1EOBCS, mono-2EOBCS, di-1EOBCS and tri-1EOBCS were white solid and stored in refrigerator before use. The others monomers mono-3EOBCS, di-mEOBCS (*m*=2, 3) and tri-mEOBCS (*m*=2, 3) were colorless or pale yellow viscous liquid with cryopreservation.

Synthesis and characterization of polymers

Conventional free radical polymerization was conducted to synthesize polymer samples. The apparent number-average molecular weights (M_n), the weight-average molecular weight (M_w) and polydispersity of all polymers are listed in Table 1. As can be seen from it, the M_n of polymers determined by GPC was higher than $5 \times 10^4 \text{ g mol}^{-1}$, demonstrating good polymerizability of the monomers. P-mono-mEOBCS, P-di-mEOBCS and P-tri-mEOBCS have good solubility in common organic solvents, such as THF and chloroform. The characterization of the polymers was performed with ^1H NMR. As an example, Fig. 1 shows the ^1H NMR spectra of monomer mono-1EOBCS and polymer P-mono-1EOBCS. Mono-1EOBCS showed characteristic resonances of vinyl group at 5.4-5.7 ppm. After polymerization, the signals disappeared completely. The adsorption peaks of P-mono-1EOBCS are quite broad, which is consistent with the expected

polymer structure.

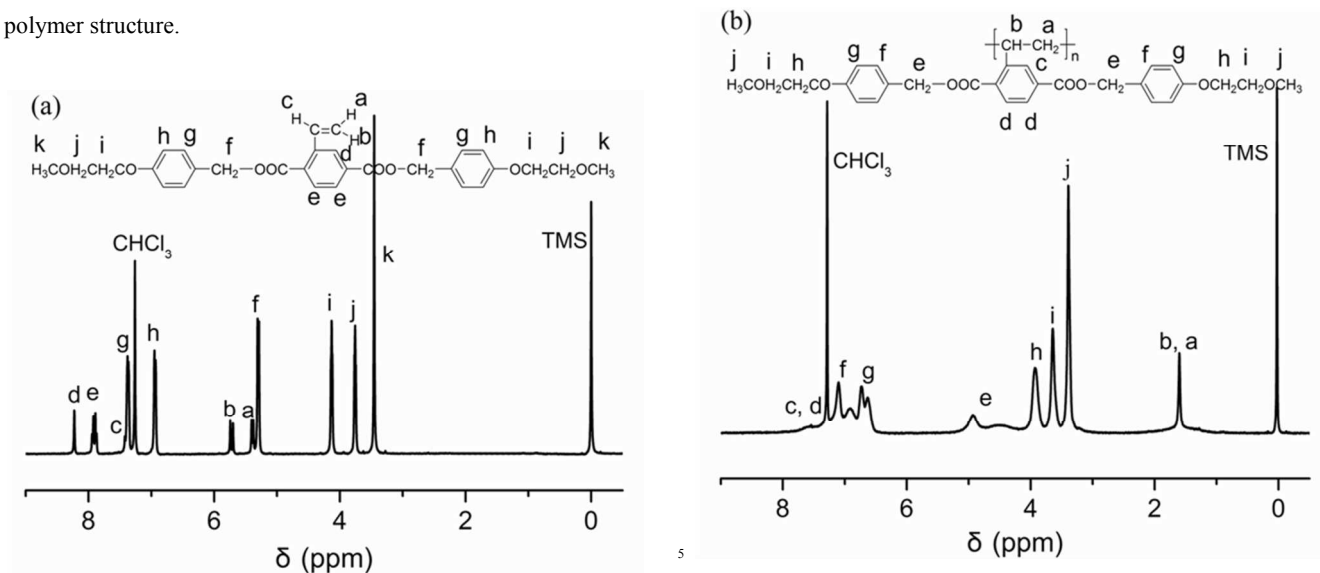


Fig.1 ^1H NMR spectra of monomer mono-1EOBCS (a) and polymer P-mono-1EOBCS (b) in CDCl_3 , respectively.

Table 1 GPC, DSC, and TGA results and thermotropic properties of polymers

Sample	Yield (%)	M_n ($\times 10^4$) ^a	M_w ($\times 10^4$) ^a	PDI ^a	DP ^b	Contour length (nm) ^c	T_g ($^\circ\text{C}$) ^d	T_d ($^\circ\text{C}$) ^e	LC ^f
P-mono-1EOBCS	85	11.1	28.2	2.54	213	43.7	27.4	372	No
P-mono-2EOBCS	83	11.6	24.7	2.13	190	38.8	- 9.8	350	No
P-mono-3EOBCS	79	7.76	16.5	2.13	111	22.6	- 34.5	348	No
P-di-1EOBCS	82	11.3	29.9	2.65	169	34.6	17.8	397	Yes
P-di-2EOBCS	80	7.59	19.7	2.60	90	18.4	- 22.6	391	Yes
P-di-3EOBCS	81	5.35	9.31	1.74	52	10.6	- 44.5	384	Yes
P-tri-1EOBCS	84	5.49	10.5	1.92	67	13.7	26.3	352	Yes
P-tri-2EOBCS	85	5.14	10.5	2.05	48	9.8	- 46.6	360	Yes
P-tri-3EOBCS	89	10.2	19.6	1.92	76	15.6	< -70	356	Yes

¹⁰ ^a Relative M_n , M_w and polydispersity (PDI) were measured by GPC using PS standards.

^b The number-average degree of polymerization (DP) calculated from M_n .

^c The contour lengths was calculated by the soft Materials studio 6.0.

^d The glass transition temperatures were measured by DSC at a heating rate of $10\text{ }^\circ\text{C min}^{-1}$ under nitrogen atmosphere during the second heating process.

^e The temperatures at 5% weight loss of the samples under nitrogen [$T_d(\text{N}_2)$] were measured by TGA heating experiments at a rate of $20\text{ }^\circ\text{C min}^{-1}$.

¹⁵ ^f The liquid crystallinity was observed by POM.

Thermal bulk properties

Fig. 2 shows that all polymers have good thermal stability, *i.e.*, the temperatures at 5% weight loss of the samples under nitrogen were about $340\text{ }^\circ\text{C}$ measured by TGA at a rate of $20\text{ }^\circ\text{C min}^{-1}$ (see Table 1). Fig. 3 shows the second heating DSC curves of P-mono-mEOBCS, P-di-mEOBCS and P-tri-mEOBCS ($m=1, 2, 3$) at a rate of $10\text{ }^\circ\text{C min}^{-1}$ under nitrogen atmosphere after eliminating the thermal history. As can be seen, the glass transitions (T_g) of all polymers (except P-tri-3EOBCS) can be observed in low temperature, and were decreased with increasing

the length of the terminal EO groups (listed in Table 1). For P-tri-3EOBCS, the T_g may be low -70° ,³¹ which could not be detected by our DSC. After T_g , no more transition peaks were seen. The phenomenon is similar to some other MJLCPs systems.

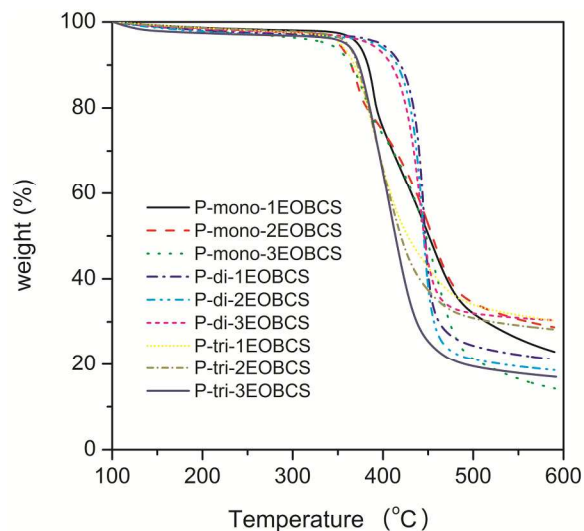


Fig. 2 TGA diagrams of polymers in N₂ at a rate of 20 °C/min.

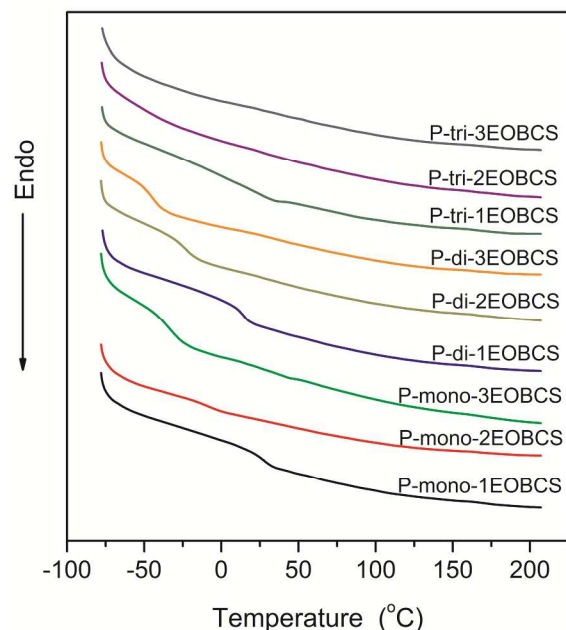


Fig. 3 DSC curves of polymers during the second heating scan at a rate of 10 °C/min under nitrogen atmosphere.

Birefringence of the polymers is observed by POM. All samples were cast from THF solution and slowly dried at room temperature, then slowly heated. The results showed that the polymers can be divided into two kinds. The first one is the P-mono-mEOBCS ($m=1, 2, 3$). No birefringence was detected by POM, implying the absence of thermotropic mesophase. The second one is P-di-mEOBCS and P-tri-mEOBCS ($m=1, 2, 3$). The samples exhibited the stable texture and some samples' POM images were shown in Fig. 4. The liquid crystalline birefringence unchanged even when heated to 300 °C. While cooled to room temperature from 300 °C, the birefringence of the sample remained unchanged, implying that the ordered structure kept unchanged upon cooling.

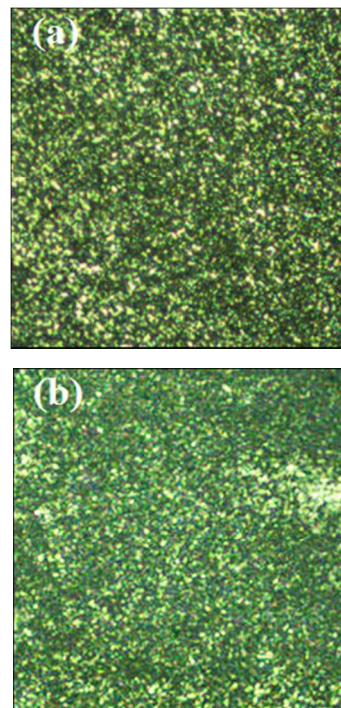


Fig. 4 Representative POM images of the texture of P-di-1EOBCS (a) and P-tri-1EOBCS (b) at 150 °C ($\times 200$).

To further characterize phase transitions and the phase structures of P-mono-mEOBCS, P-di-mEOBCS and P-tri-mEOBCS, temperature-dependent powder 1D WAXD was used. About 60 mg of the polymer was added into an aluminum foil substrate. In order to be consistent with the DSC results, the samples were heated to 250 °C, and then slowly cooled to the room temperature. For the P-mono-mEOBCS, no low-angle scattering peaks are seen in the 1D WAXD profiles during the heating and cooling processes, implying that P-mono-mEOBCS is amorphous throughout the temperature region (Seen Fig. S4, Fig. S5 and Fig. S6).

For the P-di-1EOBCS, the results are shown in Fig. 5a. As can be seen from it, in low angle, one narrow reflection peak was observed at $2\theta=4.35^\circ$ ($d=2.0$ nm), indicating the ordered structures on the nanometer scale formed. The intensity of the halo basically kept the same with the temperature elevated, *i.e.*, 210 °C. In the wide-angle region of $2\theta>10^\circ$, only an amorphous halo around 20° could be recognized. This reflected that no long range ordered structure formed *via* molecular packing was detected over the entire temperature region studied. In addition, no noticeable change could be observed during the second heating and cooling processes in 1D WAXD experiments, implying that there was no isotropic phase for P-di-1EOBCS in the temperature region from 30 to 210 °C. 1D WAXD patterns of P-di-2EOBCS and P-di-3EOBCS are similar to those of P-di-1EOBCS, as shown in the Supporting Information Fig. S7 and Fig. S8. Therefore, P-di-mEOBCS ($m=1, 2, 3$) probably forms a columnar phase.

Fig. 5b showed the structurally sensitive 1D WAXD patterns of P-tri-1EOBCS from 30 to 210 °C. Upon the second heating, higher orders of the diffractions were visible in low angle. For the sample P-tri-1EOBCS, the scattering vector ratio of the diffractions followed $1:\sqrt{3}:\sqrt{4}:\sqrt{7}$ in low angle, demonstrating

a long-range ordered hexagonal lattice. Therefore, we presumed that the sample formed a hexagonal columnar phase (Φ_H). When the sample was cooled, the hexagonal columnar phase (Φ_H) remained unchanged. Similar results were obtained from P-tri-2EOBCS and P-tri-3EOBCS (see Supporting Information Fig. S9 and Fig. S10).

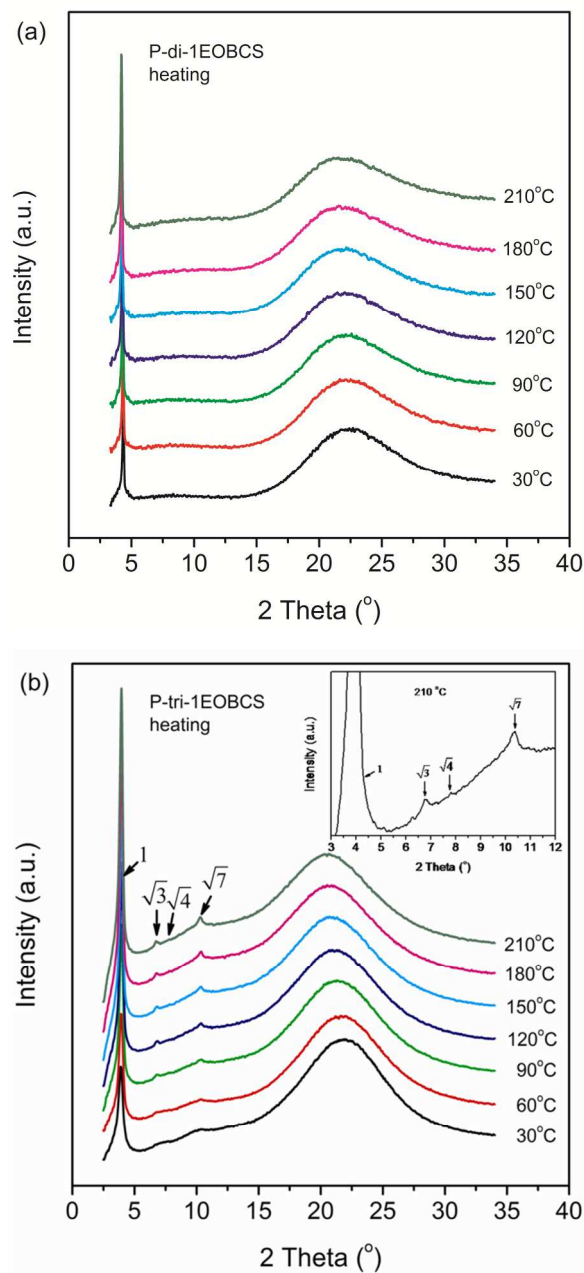


Fig.5 1D WAXD patterns of the P-di-1EOBCS (a) and the P-tri-1EOBCS (b).

Fig. 6 depicts a set of 1D WAXD patterns for this series of P-mono-mEOBCS, P-di-mEOBCS and P-tri-mEOBCS ($m=1, 2, 3$) samples obtained at 30 °C, and the data of all polymers at 30 °C was summarized in Table 2.

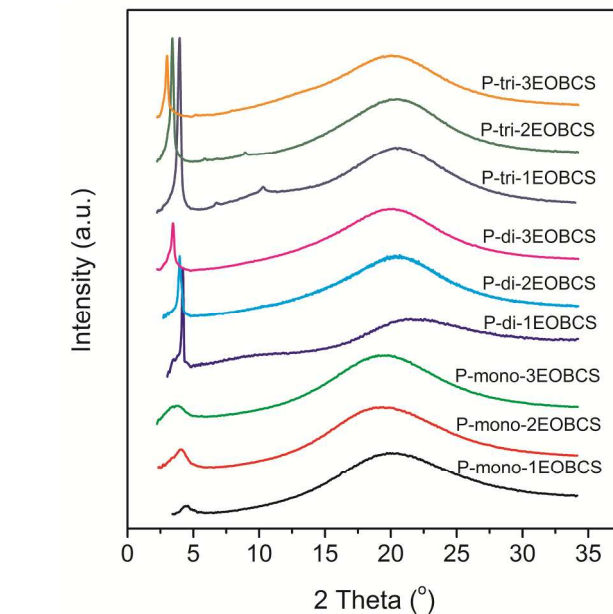


Fig.6 1D WAXD patterns of the P-mono-mEOBCS, P-di-mEOBCS and P-tri-mEOBCS ($m=1, 2, 3$).

Table 2 1D WAXD Results of polymers at 30 °C

Sample	2θ (°)	d-space (nm)	q-Ratios	Phase structure ^a	Diameter of the rod (nm)
P-mono-1EOBCS	-	-	-		
P-mono-2EOBCS	-	-	-		
P-mono-3EOBCS	-	-	-		
P-di-1EOBCS	4.37	2.02	-	Φ _H	2.33
P-di-2EOBCS	4.07	2.17	-	Φ _H	2.51
P-di-3EOBCS	3.61	2.45	-	Φ _N	2.45
P-tri-1EOBCS	3.96, 6.80, 7.80, 10.33	2.23, 1.30, 1.13, 0.86	1:√3:√4:√7	Φ _H	2.57
P-tri-2EOBCS	3.45, 5.93, 6.86, 9.12	2.56, 1.49, 1.29, 0.97	1:√3:√4:√7	Φ _H	2.95
P-tri-3EOBCS	3.08, 5.28, 6.32, 8.18	2.87, 1.67, 1.40, 1.08	1:√3:√4:√7	Φ _H	3.31

^a Φ_H: hexagonal columnar; Φ_N: columnar nematic.

2D WAXD was used to further identify the phase structures. In order to achieve chain orientation, specimens were obtained by shearing films, of the polymer at the mesophase temperature. The films were annealed at the same temperature for several hours, and were then quenched to room temperature. Fig. 7 shows the 2D WAXD patterns of P-di-1EOBCS, with the X-ray incident beam perpendicular or parallel to the shear direction. A pair of strong diffraction arcs can be seen on the equators at 2θ=4.37° (d-spacing of 2.02 nm) for P-di-1EOBCS perpendicular to the shear direction (Z or Y direction), indicating the existence of an ordered structure on the nanometer scale with lattice planes oriented primarily parallel to the shear direction (X direction). Higher-order diffractions were not observed, even with thermal annealing. This result is consistent with 1D WAXD patterns. On the other hand, scattering halos in the wide-angle region are concentrated on the meridians with rather broad azimuthal distributions. This reveals that only short-range order exists along the fiber direction. When the X-ray incident beam was parallel to the shear direction, the corresponding azimuthal intensity profiles shown in Fig. 7c exhibit six maxima with an angle of 60 separation. This indicates a hexagonal lateral packing of the cylinders with each cylinder having an average diameter of 2.33 nm for P-di-1EOBCS. Each cylinder is occupied by a single P-di-1EOBCS polymer chain. The obtained an average diameter proved to be smaller than the calculated molecular length (L=2.82 nm, L was calculated using molecular modeling software from

Material Studios 6.0) for the fully extended side-chain liquid crystalline unit of P-di-1EOBCS, suggesting that the side-chains wrapping around the polymer backbone are expected to tilt about 34° away from the cylinder long axis. Similar results were obtained from P-di-2EOBCS (see Fig. S11).

The phase structure of P-di-3EOBCS is, however, different from that of P-di-1EOBCS and P-di-2EOBCS. 2D WAXD experiments were conducted on sheared film samples of P-di-3EOBCS and the results are shown in Fig. 8. A pair of strong diffraction arcs can be seen on the equators for P-di-3EOBCS perpendicular to the shear direction (Z or Y direction). However, when the X-ray incident beam was parallel to the shear direction (Fig. 8c), we can only observe uniform diffraction circles at the low angle region (2θ=3.5°, d-spacing of 2.55 nm), suggests that the LC phase is less ordered in P-di-1EOBCS and P-di-2EOBCS and the phase structure can be assigned as a columnar nematic phase (Φ_N).

2D WAXD patterns of sheared P-tri-mEOBCS (m=1, 2, 3) are similar to P-di-1EOBCS' and the results are shown in Fig. 9, implying that the polymers formed Φ_H, which are consistent with the 1D WAXD. Therefore, the diameter of cylinder is 2.57 nm for P-tri-1EOBCS, 2.95 nm for P-tri-2EOBCS and 3.31 nm for P-tri-3EOBCS, suggesting that the diameter of the rod can be easily tuned by altering the tail length of laterally attached mesogens (Table 2).

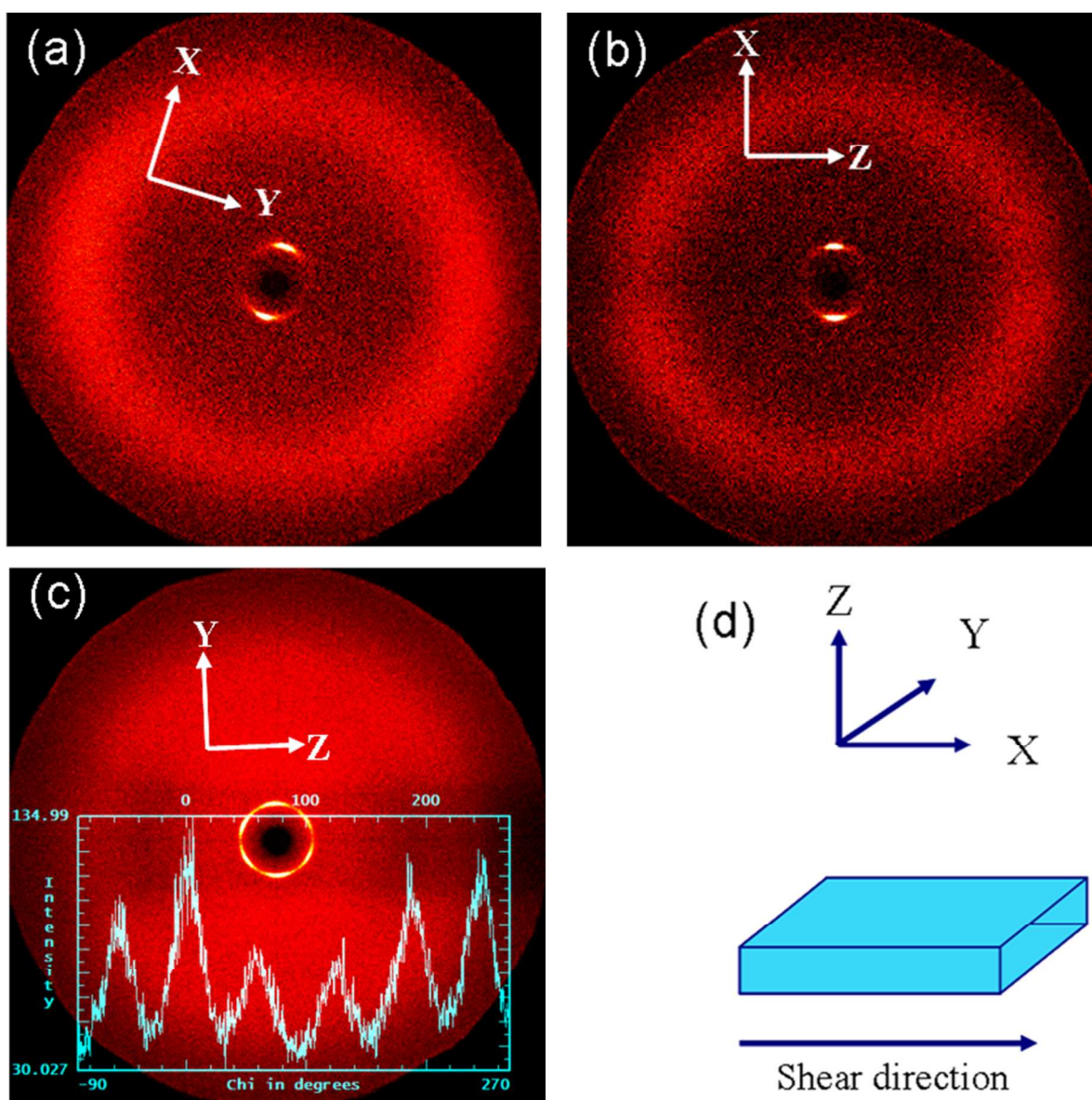


Fig.7 2D WAXD patterns of a sheared P-di-1EOBCS sample recorded with the X-ray incident beam along Z (a), Y (b), and X (c) directions and the shearing geometry (d).

5

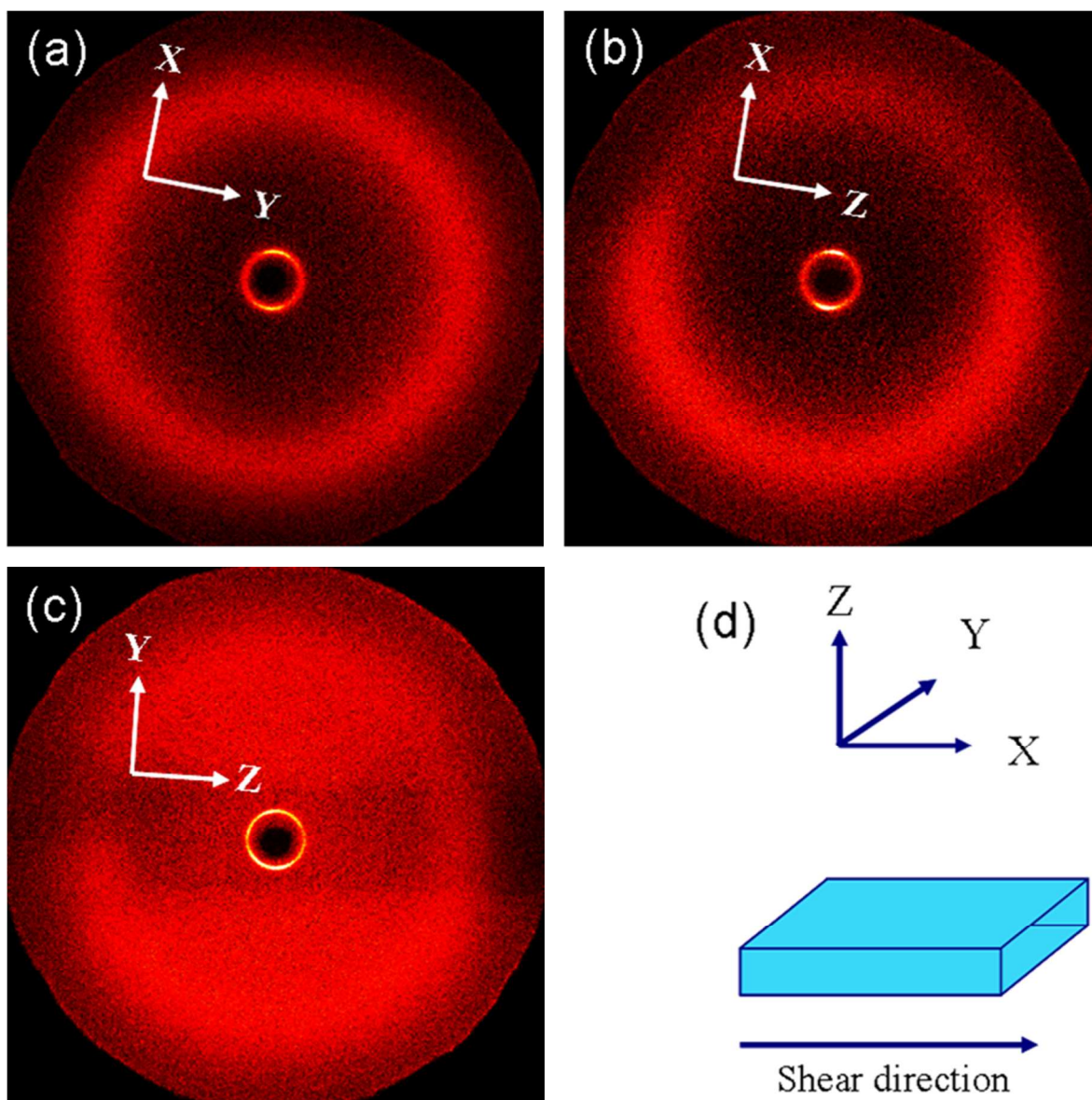


Fig.8 2D WAXD patterns of a sheared P-di-3EOBCS sample recorded with the X-ray incident beam along Z (a), Y (b), and X (c) directions and the shearing geometry (d).

5

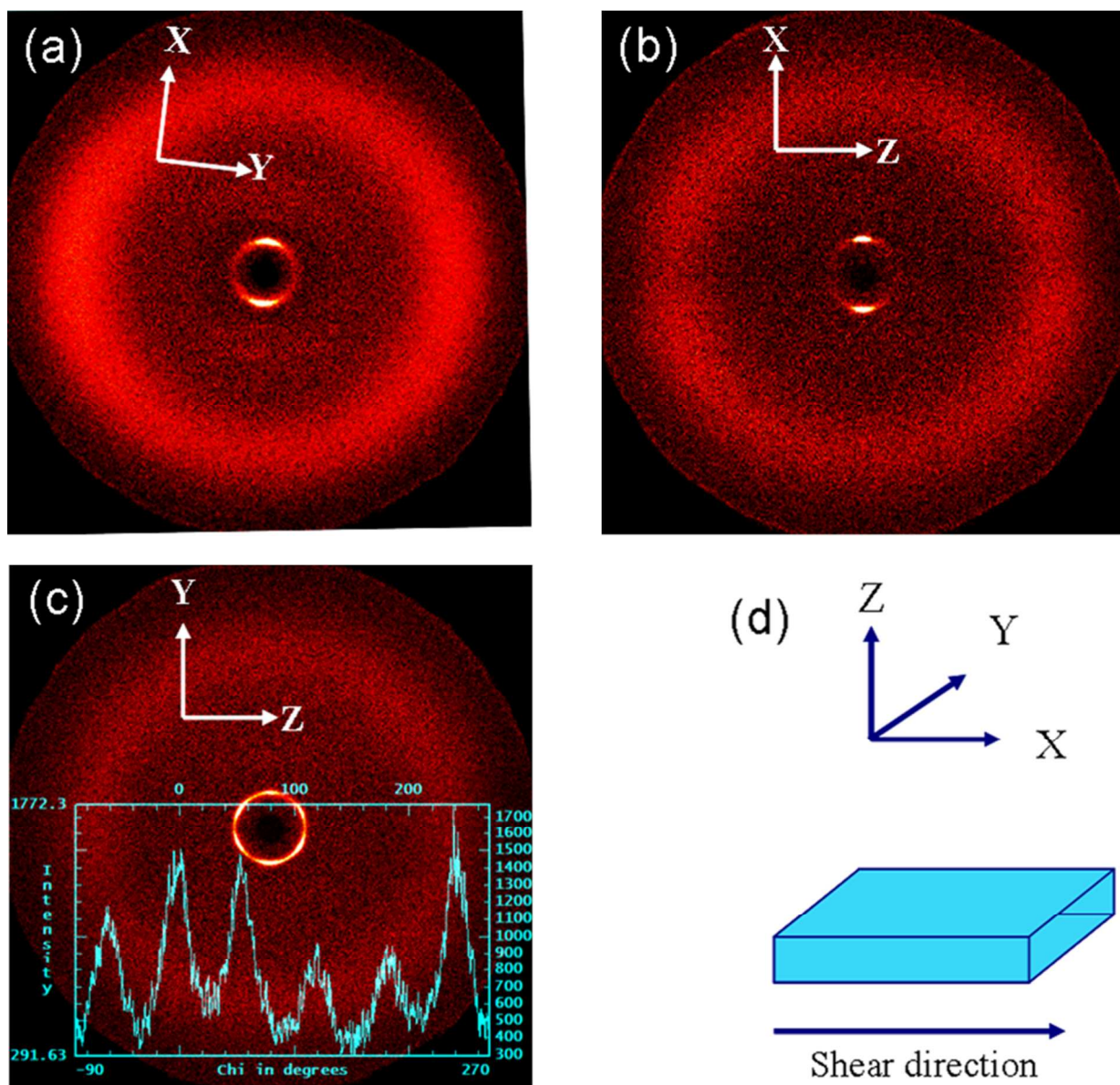


Fig.9 2D WAXD patterns of a sheared P-tri-1EOBCS sample recorded with the X-ray incident beam along Z (a), Y (b), and X (c) directions and the shearing geometry (d).

5 Based on DSC, POM, 1D/2D WAXD experiments results, the phase behaviors of all polymers are summarized in Fig. 10. From it, we can see that, one hand, contrast to the phase behavior of poly{2, 5-bis[4-methoxyoligo(oxyethylene) phenyl]oxycarbonyl} styrene} with different EO chain length
 10 which were synthesized by Chen,⁵³ the P-mono-mEOBCS could

not form the liquid crystalline phase because of the semirigid side chain (poor jacketing effect). On the other hand, the ability of mesophase formation of the polymers increased as the number of the EO terminal chain increased because the volume of side chain
 15 increased (strong jacketing effect).

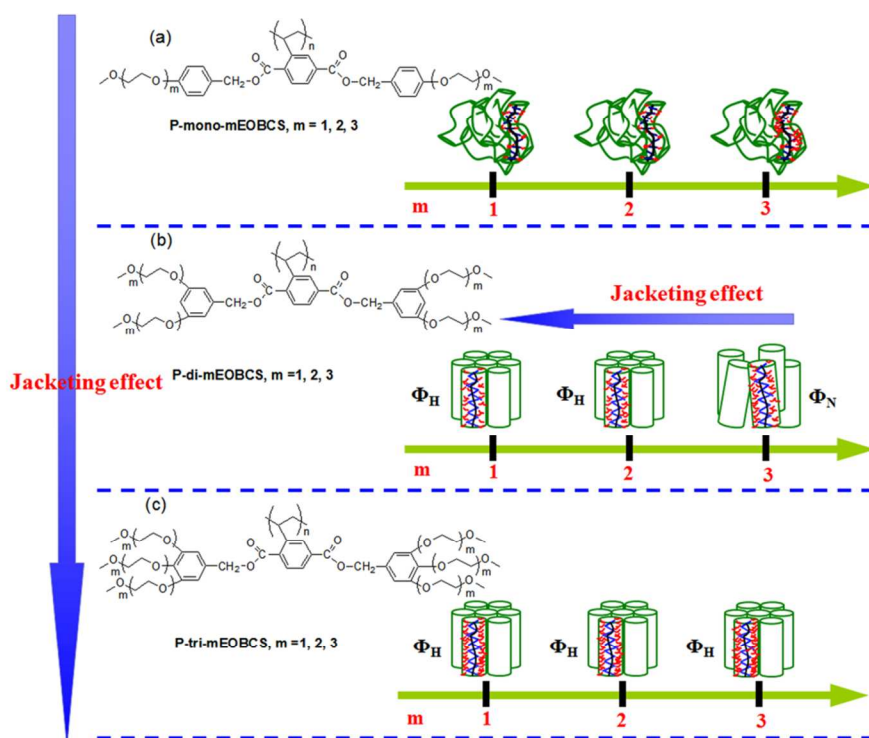


Fig.10 Schematic drawing of the thermotropic phase behaviors of P-mono-mEOBCS, P-di-mEOBCS, and P-tri-mEOBCS ($m=1, 2, 3$).

Thermoresponsive properties in water

LCST is known to arise from a subtle balance between hydrophilic and hydrophobic interactions. While at low temperature the hydrophilic part is able to counterbalance the unfavorable hydrophobic interactions and allow solubilization, a weakening of the hydrogen bonds provided by a temperature increase is enough to induce a sudden dehydration of the polymers leading to its brutal aggregation. Moreover, the balance between the hydrophobic and the hydrophilic part of the polymers can be finely tuned by increasing the numbers and length of the terminal EO groups. Indeed, in our case the hydrophilicity of the polymers can be increased by adjusting both the numbers and length of the terminal EO groups as can be seen on Fig. 11. The P-mono-mEOBCS having the fewest numbers of terminal EO chains are not water-soluble. On the opposite, P-tri-mEOBCS bearing the most numbers of terminal EO chains exhibit a high LCST in water. In between, P-di-mEOBCS ($m=2, 3$) with the appropriate number and length of terminal EO chains showed the low LCST in water.

To elucidate the thermoresponsive property of the water soluble P-mono-mEOBCS, P-di-mEOBCS and P-tri-mEOBCS in an aqueous solution, the phase transition behavior as characterized as the turbidity of the cloud point determined from the heating curve at 50% of the transmittance change. All sample solutions were visually confirmed to be optically clear prior to the turbidity measurement. The polymer concentration was 10 mg mL⁻¹. The results showed that P-mono-1EOBCS, P-mono-

2EOBCS, P-mono-3EOBCS and P-di-1EOBCS were not water-soluble. While P-di-2EOBCS, P-di-3EOBCS and P-tri-mEOBCS ($m=1, 2, 3$) exhibited LCST and the results are shown in Fig. 12. As can be seen from it, the LCST of P-di-2EOBCS and P-di-3EOBCS is 23 °C and 40 °C, respectively. With increasing the EO chain length, the LCST of P-tri-2EOBCS ($m=1, 2, 3$) increases from 22 °C to 60 °C (see Fig.11). These results clearly indicate that the length of the terminal EO chain has obvious effect on LCST. Because of the higher hydrophilicity of EO chain with $m=3$ in comparison with EO chain with $m=1$, the increase of the terminal EO chain length can make P-tri-3EOBCS more hydrophilic, resulting in higher LCST. On the other hand, although the polymers have the same the numbers of EO structural units, the polymers with the more numbers of the terminal EO chain present high LCST. For example, P-mono-3EOBCS and P-tri-1EOBCS both have six EO structural units, however, the former is not water-soluble and LCST of the later is around 22 °C. P-di-3EOBCS and P-tri-2EOBCS both have 12 EO structural units, however, the LCST of the former is lower 10 °C than the later. Those showed that a densification of the side groups (EO) is expected, leading to the formation of a more compact EO-shell that should increasingly mask the hydrophobic inner core of the macromolecule. In overall, the apparent hydrophilic character of the polymers should increase with the numbers of the terminal EO chain by congestion effect, resulting in an increase of LCST.

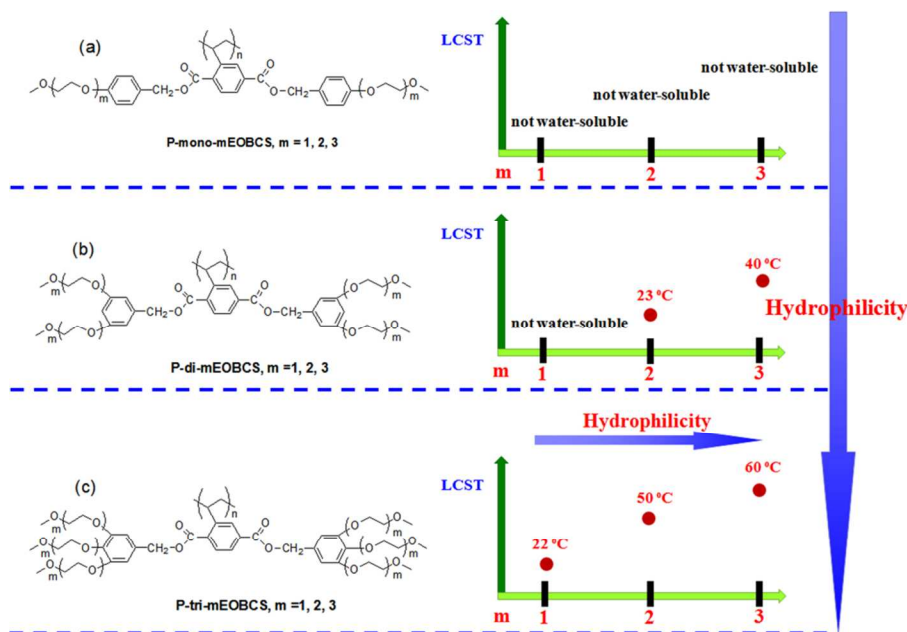


Fig.11 Evolution of hydrophilicity and water solubility for mesogen-jacket liquid crystalline polymers as a function of the number and length of EO chain.

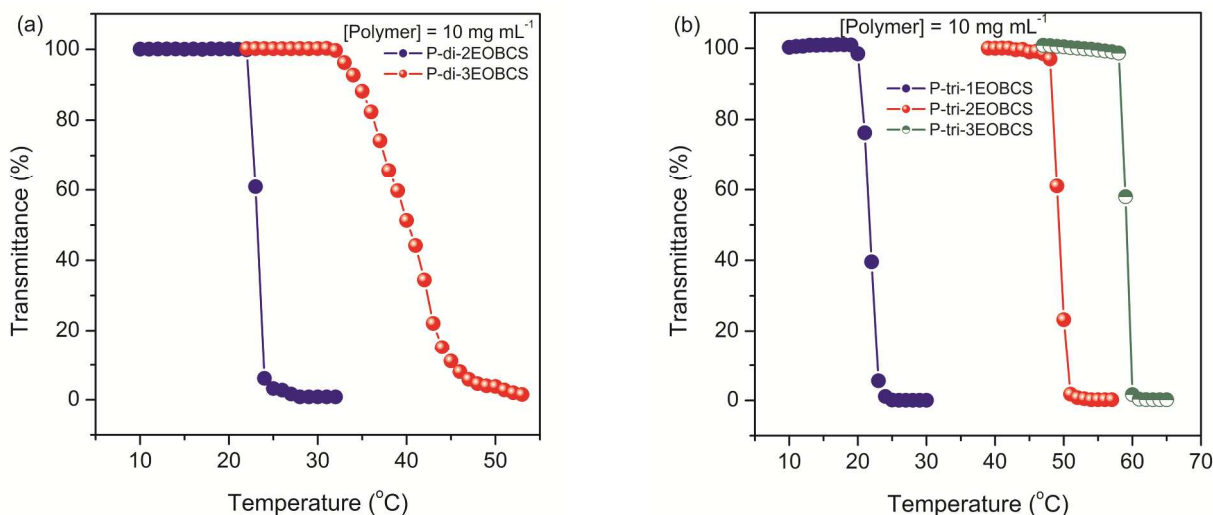


Fig.12 Effect of the numbers and length of the terminal EO chain on transmittance versus temperature for aqueous solutions (10 mg mL^{-1}) of polymers (P-di-mEOBCS ($m=2, 3$) (a) and P-tri-mEOBCS ($m=1, 2, 3$) (b)).

Fig. 13 shows the evolution of LCST with the number of terminal EO chain for the aqueous solutions of macromonomers. As can be seen from it, a very sharp transition (when heated) was observed, moreover, an increase of the number of terminal EO chain in the macromonomers causes an increase in the LCST. Because the LCST of tri-2EOBCS was too low, it was determined by the visual method and the LCST was 4°C . For the other monomers, they were insoluble. In our case, the LCST of these resultant dendronized monomers were dependent on the numbers and length of the terminal EO groups. The reasonable explanations may involve the balance of hydrophilicity and hydrophobicity in the molecular structures varied with the number of terminal EO chains. It is well-known that the ratio of the hydrophobic and hydrophilic units in the chain is crucial to

the alternation of LCST. In general, hydrophilic segments shift LCST to a higher temperature,⁵⁵ and hydrophobic units show the tendency to decrease LCST.⁵⁶ For the di-3EOBCS and tri-3EOBCS, the monomers afforded different hydrophilic and hydrophobic compositions. The tri-3EOBCS possessed more EO units that could interact with adjacent water molecules through hydrogen bonds, which enhanced the hydrophilicity of tri-3EOBCS and conducted to a higher LCST. For the tri-2EOBCS and tri-3EOBCS, the LCST increased significantly from 4°C to 57°C with the increase of the length of the terminal EO groups. Such LCST dependence on EO chain length was due to the increase of apparent hydrophilicity of the monomers because of the more EO group and a densification of the EO coverage.

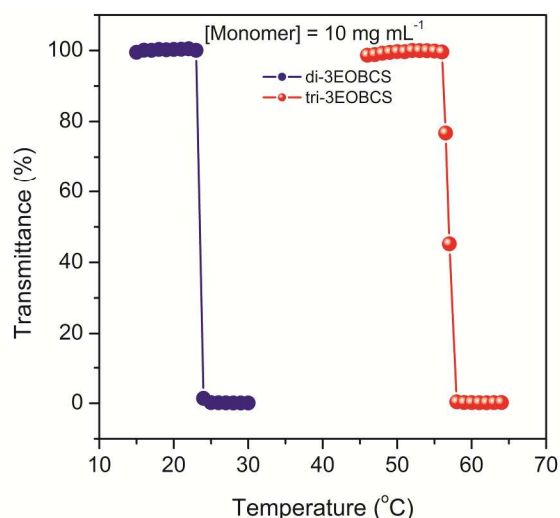


Fig.13 Effect of the numbers of the terminal EO chain on transmittance versus temperature for aqueous solutions (10 mg mL^{-1}) of monomers (di-3EOBCS and tri-3EOBCS).

5 Comparable with the change of LCST for the monomers and the corresponding polymer, a large difference (3, 16, and $46 \text{ }^\circ\text{C}$) was obtained by varying the number and length of the terminal EO chain. For example, the tri-3EOBCS showed a LCST at $57 \text{ }^\circ\text{C}$, which was only 3 degree lower than its corresponding

10 polymer P-tri-3EOBCS, while the LCST of tri-2EOBCS was below $4 \text{ }^\circ\text{C}$, which was more than 46 degree lower than that of its corresponding polymer P-tri-2EOBCS. Our monomers and polymers carry sterically demanding dendritic side groups, terminated by hydrophilic EO units. For the monomers, the side

15 groups should get enough space to move, especially at end groups, making accessible all (hydrophobic and hydrophilic) parts of macromolecule to water molecules. For the polymers, however, a densification of the EO groups is expected, resulting in the formation of a compact EO-shell. In contract with monomers, the

20 polymers showed the apparent increasing hydrophilic character, thus the LCST of polymers is higher than that of monomers. However, when the macromonomers possess the highest hydrophilic groups (EO groups), the hydrophilicity caused by densification of the EO-shell should increase slightly, leading to a

25 slight change of LCST for the monomer and the responding polymer. Another explanation for the increase of LCST may be related to a dilution effect, especially in the oligomer regime. For the same mass concentration, the polymer has a lower molar concentration, *i.e.*, a dilution of macromolecules, which is known

30 to strongly influence LCST. In our case, For the solutions (10 mg mL^{-1}) of macromonomer (tri-2EOBCS) and polymer (P-tri-2EOBCS), the molar concentration of the macromolecules decrease from 9.3 to 0.195 mM L^{-1} . All these results indicate that the observed increase of LCST for these monomers and polymers

35 should probably result from a dilution effect and an increase of macromolecular hydrophilicity (due to a densification of the dendritic coverage).

Experimental section

Materials

40 The compound of vinylterephthalic acid was synthesized using

the method previously reported. Azobisisobutyronitrile (AIBN) was purified by recrystallization from ethanol. Chlorobenzene was purified by washing with concentrated sulfuric acid to remove thiophene, followed by washing with water, and then

45 dried and distilled. Tetrahydrofuran (THF) (AR, Xilong Chemical Co., Ltd.) was heated under reflux over sodium for at least 8 h and distilled before use. 4-(Dimethylamino)pyridine (DMAP) (99%, Acros), *N,N'*-dicyclohexylcarbodiimide (DCC) (99%, Aladdin), methyl gallate (98%, Aladdin), lithium aluminium

50 hydride (97%, Aladdin), ethyleneglycol monomethyl ether (CP, Sinopharm), diethylene glycol monomethyl ether (CP, Sinopharm), methyl *p*-hydroxybenzoate (CP, Sinopharm), tosyl chloride ($\geq 98.5\%$, Sinopharm), methyl 3, 5-dihydroxybenzoate (99%, Shengbaoxiang), triethylene glycol monomethyl ether

55 (98%, TCI), and other reagents were used as received without further purification.

Characterization

Nuclear magnetic resonance (NMR). ^1H and ^{13}C NMR spectroscopy were recorded on a BRUKER ARX 400

60 spectrometer at room temperature with deuterated chloroform as the solvent and tetramethylsilane (TMS) as the internal standard.

Mass spectrometry (MALDI-ToF). MALDI-ToF analysis was performed with a Bruker Aupoflex III equipped with a neodymium-doped yttrium aluminium garnet laser (Nd:YAG).

65 **Gel permeation chromatography (GPC).** The number-average molecular weights (M_n), weight-average molecular weight (M_w), and polydispersity index (PDI, M_w/M_n) were determined by DMF gel permeation chromatography (GPC) at $80 \text{ }^\circ\text{C}$. The GPC setup comprised three Polymer Laboratories PL gel

70 $5 \mu\text{L MIXED-D}$ columns ($300 \times 7.5 \text{ mm}$) in series with a Viscotek TriSEC model 302 refractive detector. The flow rate was 1.0 mL min^{-1} , and the mobile phase contained 10 mmol LiBr . Five nearmonodisperse polystyrene standards ($M_n = 0.2\text{--}400.0 \text{ kg mol}^{-1}$) were used for calibration. Data were analyzed using Viscotek

75 TriSEC 3.0 software.

Thermogravimetric analysis (TGA). The TGA of polymers was performed on a TA SDT 2960 instrument in nitrogen atmosphere at a heating rate of $20 \text{ }^\circ\text{C min}^{-1}$ from ambient temperature to $600 \text{ }^\circ\text{C}$. All the samples were preheated at $100 \text{ }^\circ\text{C}$

80 to remove any trace of water.

Differential scanning calorimetry (DSC). The DSC examination was carried out on a TA-Q100 instrument in nitrogen atmosphere. Samples with a typical mass of about 5 mg were encapsulated in sealed aluminum pans. The temperature and

85 heat flow were calibrated using standard materials (indium and zinc) at a cooling and heating rates of $10 \text{ }^\circ\text{C min}^{-1}$.

Polarizing optical microscope (POM). LC texture of the polymers was examined under POM (Leica DM-LM-P) equipped with a Mettler-Toledo hot stage (FP82HT).

90 **One-dimensional wide-angle X-ray diffraction (1D WAXD).** 1D WAXD powder experiments were performed on a BRUKER AXS D8 Advance diffractometer with a 40 kV FL tubes as the X-ray source (Cu $K\alpha$) and the LYNXEYE_XE detector. The sample stage was set horizontally. Background scattering was recorded

95 and subtracted from the sample patterns. A temperature control unit (Anton Paar TCU 110) in conjunction with the diffractometer was utilized to study the structure evolutions as a function of temperature. The heating and cooling rates in the 1D

WAXD experiments were $10\text{ }^{\circ}\text{C min}^{-1}$.

Two-dimensional wideangle X-ray diffraction (2D WAXD).

2D WAXD was carried out using a BRUKER AXS D8 Discover diffractometer with a 40 kV FL tubes as the X-ray source (Cu $K\alpha$) and the VANTEC 500 detector. The oriented samples were prepared by mechanically shearing from the LC phase when applicable. The point-focused X-ray beam was aligned either perpendicular or parallel to the mechanical shearing direction. For both the 1D and 2D WAXD experiments, the background scattering was recorded and subtracted from the sample patterns.

UV-visible spectrophotometer (UV-vis). Turbidity measurements were carried out on a PerkinElmer Lambda 25 spectrophotometer equipped with a Peltier temperature-control programmer ($\pm 0.1\text{ }^{\circ}\text{C}$). The cloud point was determined by spectrophotometric detection of the changes in transmittance at $\lambda=500\text{ nm}$ of the aqueous polymer solutions. The heating rate was $1.0\text{ }^{\circ}\text{C min}^{-1}$ in steps of $1\text{ }^{\circ}\text{C}$ followed by a 5 min period of constant temperature to ensure equilibration. The cloud point was defined as the temperature corresponding to a 50% decrease in optical transmittance.

Synthesis of monomers and polymers

The synthetic route of monomers and the corresponding polymers (P-mono-mEOBCS P-di-mEOBCS and P-tri-mEOBCS, $m=1, 2, 3$) is shown in Scheme 2. The experimental details are described as follows using 2, 5-bis[4-(methoxyethoxybenzyl)oxycarbonyl]styrene (mono-1EOBCS) as an example.

Synthesis of 2-methoxyethyl 4-methylbenzenesulfonate.

Tosyl chloride (52.5 g, 0.275 mol) and 19.0 g of 2-methoxyethanol (0.25 mol) were dissolved in 25 mL of THF at room temperature. Afterward, the mixture was cooled in an ice bath, and 100 mL (3.75 mol L^{-1}) of NaOH solution was added dropwise under stirring for 2 h. Then the reaction continued for 5 h. Later, the solution was stirred for 15 min together with a mixture of 250 g of ice and 80 mL of concentrated HCl. The aqueous phase was separated and extracted with methylene chloride. The combined organic phases were washed with water three times and dried with magnesium sulfate, and then condensed solvent to yield a colorless liquid (37.5 g, 65%). $^1\text{H NMR}$ (CDCl_3 , TMS), δ : 7.82-7.80 (d, 2H, Ar-H); 7.35-7.33 (d, 2H, Ar-H); 4.17-4.15 (t, 2H, $-\text{SO}_3\text{CH}_2-$); 3.59-3.58 (t, 2H, $-\text{CH}_2\text{OCH}_3$); 3.31 (s, 3H, $-\text{OCH}_3$); 2.45 (s, 3H, Ar- CH_3) (Fig. S1).

Synthesis of methyl 4-(2-methoxyethoxy) benzoate.

Methyl 4-hydroxybenzoate (10.0 g, 66 mmol), 2-methoxyethyl 4-methylbenzene sulfonate (15.3 g, 66 mmol) were dissolved in 1, 4-dioxane (150 mL) and refluxed for 0.5 h. Then K_2CO_3 (35.97 g, 0.26 mol) and 1, 4-dioxane (50 mL) were added, and the reaction was refluxed for a period time. The reaction was found to be completed by thin-layer chromatography (TLC). The reaction mixture was precipitated into a large amount of ice water, and was filtrated followed by drying under vacuum at $40\text{ }^{\circ}\text{C}$ for about 24 h. The crude product was recrystallized in petroleum ether/tetrahydrofuran to yield a white solid product (8.78 g, yield: 64%). $^1\text{H NMR}$ (CDCl_3 , TMS), δ : 7.99-7.97 (d, 2H, Ar-H); 6.95-6.93 (d, 2H, Ar-H); 4.17 (t, 2H, ArOCH_2-); 3.88 (s, 3H, $-\text{COOCH}_3$); 3.77 (t, 2H, $\text{ArOCH}_2\text{CH}_2-$); 3.46 (s, 3H, $-\text{OCH}_3$) (Fig. S2).

Synthesis of [4-(2-methoxyethoxy)phenyl] methanol. LiAlH_4

(1.45 g, 38 mmol) was suspended in dry THF (20 mL), and the solution of methyl 4-(2-methoxyethoxy)benzoate (8.0 g, 38 mmol) in THF (100 mL) was added slowly dropwise at room temperature. After the addition was complete, the mixture was reacted for further 2 h at room temperature. The reaction was found to be complete by TLC. Water was then added slowly with vigorous stirring to terminate the reaction, and then diluted HCl was added to dissolve the precipitate. The product was extracted with CH_2Cl_2 . The extracts were dried over anhydrous MgSO_4 , and condensed to yield a white solid (6.0 g, 87%). $^1\text{H NMR}$ (CDCl_3 , TMS), δ : 7.32-7.30 (d, 2H, Ar-H); 6.92-6.90 (d, 2H, Ar-H); 4.57 (s, 2H, ArCH_2OH); 4.13 (t, 2H, ArOCH_2-); 3.76 (t, 2H, $-\text{CH}_2\text{OCH}_3$); 3.46 (s, 3H, $-\text{OCH}_3$) (Fig. S3).

Synthesis of 2, 5-bis[4-(methoxyethoxybenzyl)oxycarbonyl]styrene (mono-1EOBCS).

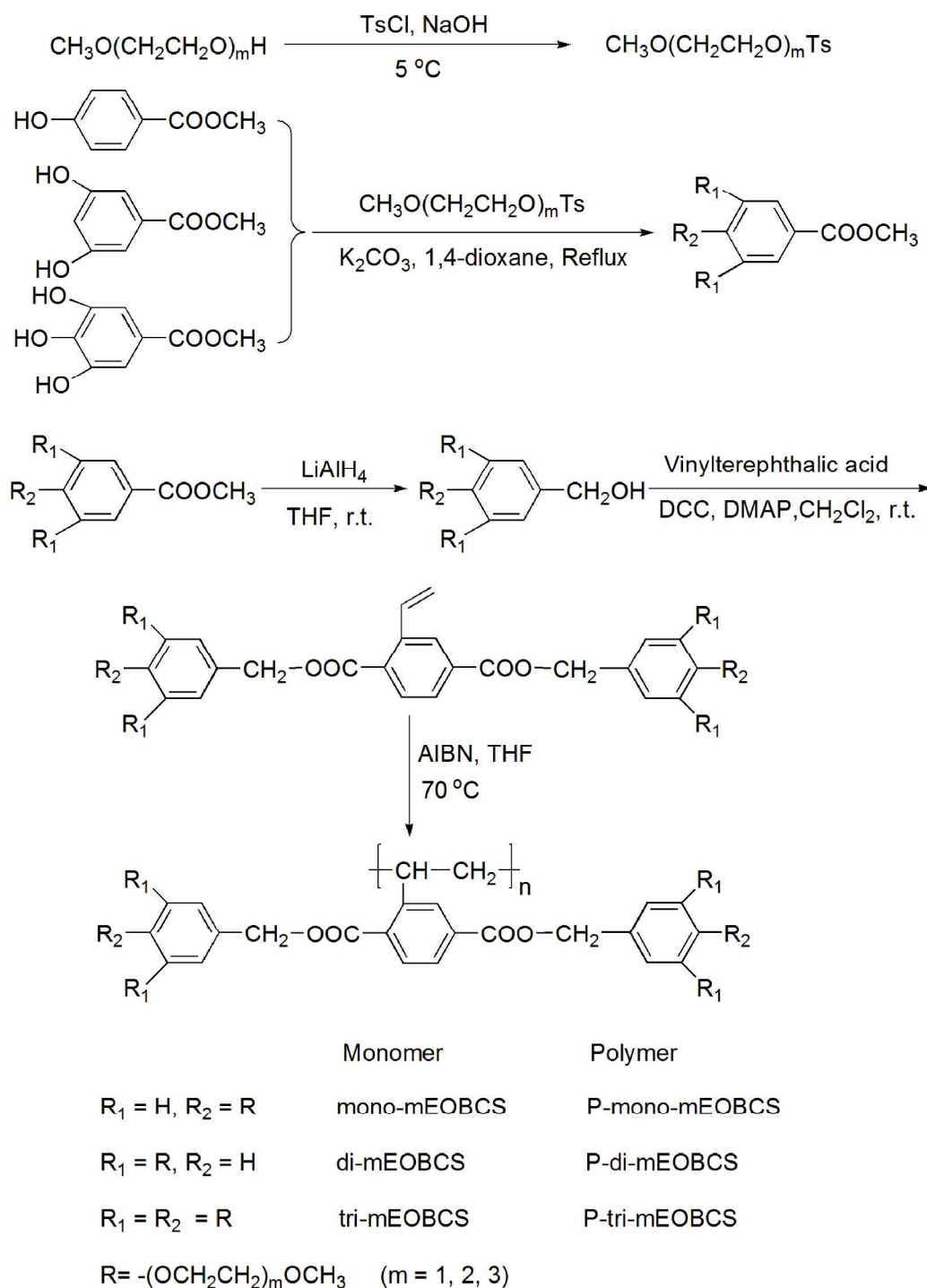
[4-(2-Methoxyethoxy)phenyl] methanol (2.71 g, 15 mmol), *N, N'*-dicyclohexylcar (DCC) (3.07 g, 15 mmol), 4-(dimethylamino)pyridine (DMAP) (0.18 g, 1.5 mmol), and vinylterephthalic acid (1.5 g, 8 mmol) were dissolved in 60 mL of dichloromethane. The mixture was stirred for 24 h at room temperature. Then the salt was removed by filtration and the product was extracted with CH_2Cl_2 . The extracts were dried over anhydrous MgSO_4 , and condensed to remove the solvent. Afterwards, the crude product was purified by column chromatography (silica gel, acetone/petroleum ether 1/5), and recrystallised from acetone/petroleum ether to obtain the monomer (3.2 g, 74%). $^1\text{H NMR}$ (CDCl_3 , TMS), δ : 8.22 (s, 1H, Ar-H); 7.94-7.87 (m, 2H, Ar-H); 7.42 (m, 1H, $-\text{CH}=\text{CH}_2$); 7.38-7.36 (d, 4H, Ar-H); 6.95-6.93 (d, 4H, Ar-H); 5.74-5.70 (d, 1H, $-\text{CH}=\text{CH}_2$); 5.40-5.38 (d, 1H, $-\text{CH}=\text{CH}_2$); 5.31-5.29 (d, 4H, $-\text{COOCH}_2-$); 4.13-4.11 (t, 4H, ArOCH_2-); 3.76 (t, 4H, $-\text{CH}_2\text{OCH}_3$); 3.45 (s, 6H, $-\text{OCH}_3$). $^{13}\text{C NMR}$ (CDCl_3 , TMS), δ : 59.18 ($-\text{OCH}_3$); 66.93-66.96 ($-\text{COOCH}_2-$); 67.37 (ArOCH_2-); 70.99 ($-\text{CH}_2\text{OCH}_3$); 114.75 (aromatic C ortho to $-\text{OCH}_2\text{CH}_2\text{OCH}_3$); 117.67 ($-\text{CH}=\text{CH}_2$); 127.99 (aromatic C ortho to $-\text{CH}_2-$); 128.12-128.36 (aromatic C ortho to $-\text{C}=\text{O}$); 130.08-131.30 (aromatic C- CH_2-); 132.49-133.24 (aromatic C- $-\text{C}=\text{O}$); 134.81 ($-\text{CH}=\text{CH}_2$); 139.58 (aromatic C- $-\text{CH}=\text{CH}_2$); 159.00 (aromatic C- $-\text{OCH}_2\text{CH}_2\text{OCH}_3$); 165.64-166.62 ($\text{C}=\text{O}$). Mass Spectrometry (MS) (m/z) [M] Calcd for $\text{C}_{30}\text{H}_{32}\text{O}_8$, 520.6; found, 520.2.

Synthesis of mono-mEOBCS ($m=2$ and 3), di-mEOBCS ($m=1, 2, 3$), and (tri-mEOBCS) ($m=1, 2, 3$).

All the other monomers were synthesized and characterized similarly. The characterization data of other monomers were showed in Supporting Information.

Polymerization.

All polymers were obtained by conventional solution radical polymerization (see Scheme 2). A typical polymerization procedure was carried out as follows: for example, mono-1EOBCS (0.5 g, 0.96 mmol), 158 μL of 0.01 M tetrahydrofuran solution of AIBN, and tetrahydrofuran (1.3 mL) were transferred into a polymerization tube. After three freeze-pump-thaw cycles, the tube was sealed off under vacuum. Polymerization was carried out at $70\text{ }^{\circ}\text{C}$ for a certain period of time. The tube was then opened, and the reaction mixture was diluted with THF (10 mL), and then reprecipitated in petroleum ether. After purification, the polymers were dried to a constant weight.



Scheme 2 The synthesis of monomers and corresponding polymers.

Conclusions

In summary, we have successfully synthesized a series of MJLCPs with different length and numbers of EO terminal groups, P-mono-mEOBCS, P-di-mEOBCS, and P-tri-mEOBCS by free radical polymerization. Combining 1D/2D WAXD results with POM and DSC observations, P-mono-mEOBCS ($m=1, 2, 3$) presented the isotropic phase because of the poor jacketing effect. When increased the number of EO terminal groups, the P-di-

mEOBCS and P-tri-mEOBCS showed the stable Φ_H because of the strong jacketing effect, beside P-di-3EOBCS formed the Φ_N . Based on the hydrophilicity-hydrophobicity balance, P-di-2EOBCS, P-di-3EOBCS and P-tri-mEOBCS ($m=1, 2, 3$) exhibited LCST, while P-mono-1EOBCS, P-mono-2EOBCS, P-mono-3EOBCS and P-di-1EOBCS were not water-soluble. One hand, with increasing the length of EO terminal chain, the LCST of the polymers increased. On the other hand, although the polymers have the same the numbers of EO structural units, the

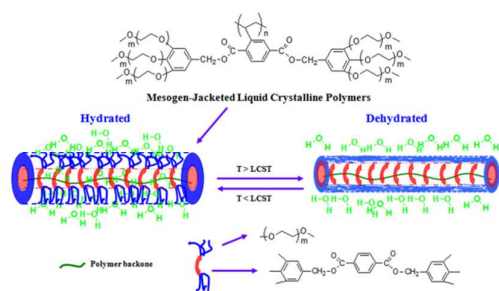
polymers with the more numbers of the terminal EO present a high LCST because of the formation of a more compact EO-shell that should increasingly mask the hydrophobic inner core of the macromolecule. Since MJLCPs is generally expected to have a rod-like structure because of jacketing effect, it may allow for the development of novel smart materials having stimuli responsive properties due to their unique properties like main-chain stiffness. More researches on the structure and conformation of the polymers in solution are ongoing and will be reported later.

10 Acknowledgements

This research was financially supported by Specialized Research Fund for the Doctoral Program of Higher Education (20114301130001), the Innovation Platform Open Foundation of University of Hunan Province (10k067), the National Nature Science Foundation of China (51073131, 21174117).

Notes and references

- 1 E. S. Gil and S. M. Hudson, *Prog. Polym. Sci.*, 2004, **29**, 1173-1222.
- 2 H. I. Lee, J. Pietrasik, S. S. Sheiko and K. Matyjaszewski, *Prog. Polym. Sci.*, 2010, **35**, 24-44.
- 3 S. Dai, P. Ravi and K. C. Tam, *Soft Matter*, 2009, **5**, 2513-2533.
- 4 F. D. Jochum and P. Theato, *Chem. Soc. Rev.*, 2013, **42**, 7468-7483.
- 5 W. H. Chiang, V. T. Ho, W. C. Huang, Y. F. Huang, C. S. Chern and H. C. Chiu, *Langmuir*, 2012, **28**, 15056-15064.
- 6 M. A. C. Stuart, W. T. S. Huck, J. Genzer, M. Muller, C. Ober, M. Stamm, G. B. Sukhorukov, I. Szleifer, V. V. Tsukruk, M. Urban, F. Winnik, S. Zauscher, I. Luzinov and S. Minko, *Nat. Mater.*, 2010, **9**, 101-113.
- 7 Y. Oda, S. Kanaoka and S. Aoshima, *J. Polym. Sci., Part A: Polym. Chem.*, 2010, **48**, 1207-1213.
- 8 N. González, C. Elvira and J. S. Román, *Macromolecules*, 2005, **38**, 9298-9303.
- 9 J. Huang and A. Heise, *Chem. Soc. Rev.*, 2013, **42**, 7373-7390.
- 10 N. Liu, M. Yi, M. L. Zhai, J. Li and H. Ha, *Radiat. Phys. Chem.*, 2001, **61**, 69-73.
- 11 Y. R. Ren, X. S. Jiang and J. Yin, *J. Polym. Sci., Part A: Polym. Chem.*, 2009, **47**, 1292-1297.
- 12 A. Schmalz, M. Hanisch, H. Schmalz and A. H. E. Müller, *Polymer*, 2010, **51**, 1213-1217.
- 13 S. S. Zhang, C. Y. Chen and Z. B. Li, *Chin. J. Polym. Sci.*, 2013, **31**, 201-210.
- 14 A. H. Soeriyadi, G. Z. Li, S. Slavin, M. W. Jones, C. M. Amos, C. R. Becer, M. R. Whittaker, D. M. Haddleton, C. Boyer and T. P. Davis, *Polym. Chem.*, 2011, **2**, 815-822.
- 15 H. Cheng, L. Shen and C. Wu, *Macromolecules*, 2006, **39**, 2325-2329.
- 16 Y. Maeda, T. Higuchi and I. Ikeda, *Langmuir*, 2000, **16**, 7503-7509.
- 17 Y. Ono and T. Shikata, *J. Am. Chem. Soc.*, 2006, **128**, 10030-10031.
- 18 J. Xu, J. Ye and S. Y. Liu, *Macromolecules*, 2007, **40**, 9103-9110.
- 19 W. Q. Chen, H. Wei, S. L. Li, J. Feng, J. Nie, X. Z. Zhang and R. X. Zhuo, *Polymer*, 2008, **49**, 3965-3972.
- 20 M. S. Thompson, T. P. Vadala, M. L. Vadala, Y. Lin and J. S. Riffle, *Polymer*, 2008, **49**, 345-373.
- 21 X. W. Jiang, M. R. Smith III and G. L. Baker, *Macromolecules*, 2008, **41**, 318-324.
- 22 T. Ishizone, A. Seki, M. Hagiwara, S. Han, H. Yokoyama, A. Oyane, A. Deffieux and S. Carloti, *Macromolecules*, 2008, **41**, 2963-2967.
- 23 F. J. Hua, X. G. Jiang, D. J. Li and B. Zhao, *J. Polym. Sci., Part A: Polym. Chem.*, 2006, **44**, 2454-2467.
- 24 X. H. Fu, Y. Shen, W. X. Fu and Z. B. Li, *Macromolecules*, 2013, **46**, 3753-3760.
- 25 S. Aoshima, H. Oda and E. Kobayashi, *J. Polym. Sci., Part A: Polym. Chem.*, 1992, **30**, 2407-2413.
- 26 B. Zhao, D. J. Li, F. J. Hua and D. R. Green, *Macromolecules*, 2005, **38**, 9509-9517.
- 27 G. X. Hu, W. Li, Y. L. Hu, A. Q. Xu, J. T. Yan, L. X. Liu, X. C. Zhang, K. Liu and A. F. Zhang, *Macromolecules*, 2013, **46**, 1124-1132.
- 28 N. Sakai, M. Jin, S. I. Sato, T. Satoh and T. Kakuchi, *Polymer Chemistry*, 2014.
- 29 N. Merlet-Lacroix, J. Rao, A. Zhang, A. D. Schlüter, S. Bolisetty, J. Ruokolainen and R. Mezzenga, *Macromolecules*, 2010, **43**, 4752-4760.
- 30 A. J. Soininen, E. Kasëmi, A. D. Schlüter, O. Ikkala, J. Ruokolainen and R. Mezzenga, *J. Am. Chem. Soc.*, 2010, **132**, 10882-10890.
- 31 J. Roeser, F. Moingeon, B. Heinrich, P. Masson, F. Arnaud-Neu, M. Rawiso and S. Méry, *Macromolecules*, 2011, **44**, 8925-8935.
- 32 J. Roeser, B. Heinrich, C. Bourgogne, M. Rawiso, S. Michel, V. Hubscher-Bruder, F. Arnaud-Neu and S. Méry, *Macromolecules*, 2013, **46**, 7075-7085.
- 33 J. G. Rudick and V. Percec, *Acc. Chem. Res.*, 2008, **41**, 1641-1652.
- 34 B. M. Rosen, C. J. Wilson, D. A. Wilson, M. Peterca, M. R. Imam and V. Percec, *Chem. Rev.*, 2009, **109**, 6275-6540.
- 35 V. Percec, H. J. Sun, P. Leowanawat, M. Peterca, R. Graf, H. W. Spiess, X. Zeng, G. Ungar and P. A. Heiney, *J. Am. Chem. Soc.*, 2013, **135**, 4129-4148.
- 36 V. Percec, P. Leowanawat, H. J. Sun, O. Kulikov, C. D. Nusbaum, T. M. Tran, A. Bertin, D. A. Wilson, M. Peterca, S. Zhang, N. P. Kamat, K. Vargo, D. Mook, E. D. Johnston, D. A. Hammer, D. J. Pochan, Y. Chen, Y. M. Chabre, T. C. Shiao, M. Bergeron-Brlek, S. André, R. Roy, H. J. Gabius and P. A. Heiney, *J. Am. Chem. Soc.*, 2013, **135**, 9055-9077.
- 37 W. Li, D. Wu, A. D. Schlüter and A. Zhang, *J. Polym. Sci., Part A: Polym. Chem.*, 2009, **47**, 6630-6640.
- 38 W. Li, A. F. Zhang, K. Feldman, P. Walde and A. D. Schlüter, *Macromolecules*, 2008, **41**, 3659-3667.
- 39 S. Bolisetty, C. Schneider, F. Polzer, M. Ballauff, W. Li, A. F. Zhang and A. D. Schlüter, *Macromolecules*, 2009, **42**, 7122-7128.
- 40 Q. F. Zhou, H. M. Li and X. D. Feng, *Macromolecules*, 1987, **20**, 233-234.
- 41 Q. F. Zhou, X. L. Zhu and Z. Q. Wen, *Macromolecules*, 1989, **22**, 491-493.
- 42 Y. F. Zhu, X. L. Guan, Z. H. Shen, X. H. Fan and Q. F. Zhou, *Macromolecules*, 2012, **45**, 3346-3355.
- 43 S. Chen, C. K. Jie, H. L. Xie and H. L. Zhang, *J. Polym. Sci., Part A: Polym. Chem.*, 2012, **50**, 3923-3935.
- 44 S. T. Sun, H. Tang, P. Y. Wu and X. H. Wan, *Phys. Chem. Chem. Phys.*, 2009, **11**, 9861-9870.
- 45 H. L. Xie, S. J. Wang, G. Q. Zhong, Y. X. Liu, H. L. Zhang and E. Q. Chen, *Macromolecules*, 2011, **44**, 7600-7609.
- 46 Z. G. Zhu, J. G. Zhi, A. H. Liu, J. X. Cui, H. Tang, W. Q. Qiao, X. H. Wan and Q. F. Zhou, *J. Polym. Sci., Part A: Polym. Chem.*, 2007, **45**, 830-847.
- 47 L. Weng, J. J. Yan, H. L. Xie, G. Q. Zhong, S. Q. Zhu, H. L. Zhang and E. Q. Chen, *J. Polym. Sci., Part A: Polym. Chem.*, 2013, **51**, 1912-1923.
- 48 X. F. Chen, Z. H. Shen, X. H. Wan, X. H. Fan, E. Q. Chen, Y. G. Ma and Q. F. Zhou, *Chem. Soc. Rev.*, 2010, **39**, 3072-3101.
- 49 C. A. Yang, G. Wang, H. L. Xie and H. L. Zhang, *Polymer*, 2010, **51**, 4503-4510.
- 50 Y. D. Xu, Q. Yang, Z. H. Shen, X. F. Chen, X. H. Fan and Q. F. Zhou, *Macromolecules*, 2009, **42**, 2542-2550.
- 51 P. Gopalan, L. Andruzzi, X. F. Li and C. K. Ober, *Macromol. Chem. Phys.*, 2002, **203**, 1573-1583.
- 52 G. L. Jiang, H. H. Cai, Z. H. Shen, X. H. Fan and Q. F. Zhou, *J. Polym. Sci., Part A: Polym. Chem.*, 2013, **51**, 557-564.
- 53 X. C. Liang, X. F. Chen, C. Y. Li, Z. H. Shen, X. H. Fan and Q. F. Zhou, *Polymer*, 2010, **51**, 3693-3705.
- 54 C. Ye, H. L. Zhang, Y. Huang, E. Q. Chen, Y. L. Lu, D. Y. Shen, X. H. Wan, Z. H. Shen, S. Z. D. Cheng and Q. F. Zhou, *Macromolecules*, 2004, **37**, 7188-7196.
- 55 M. Shibayama, T. Tanaka and C. C. Han, *J. Chem. Phys.*, 1992, **97**, 6842-6854.
- 56 Y. G. Takei, T. Aoki, K. Sanui, N. Ogata, T. Okano and Y. Sakurai, *Bioconjugate Chem.*, 1993, **4**, 341-346.

Table of contents entry:**Highlight**

- The influence of the number and length of EO terminal groups for MJLCPs on phase structure and thermoresponsive behavior.